RADC-TR-72-204
Final Technical Report
July 1972

EFFECTS OF TURBULENCE INSTABILITIES ON LASER PROPAGATION

RCA LABORATORIES

SPONSORED BY
DEFENSE ADVANCED RESEARCH PROJECTS AGENCY
ARPA ORDER NO. 1279

The views and conclusions contained in this document are those of the authors and should not be interpreted as necessarily representing the official policies, either expressed or implied, of the Defense Advanced Research Projects Agency or the U.S. Government.

ROME AIR DEVELOPMENT CENTER
AIR FORCE SYSTEMS COMMAND
GRIFFISS AIR FORCE BASE, NEW YORK

Unclassified
Security Classification

DOCUMENT CONTROL DATA - R & D

(Security classification of title, body of abstract and indexing annotation must be entered when the overall report is classified)

1. ORIGINATING ACTIVITY (Corporate author)	2a. REPORT SECURITY CLASSIFICATION
RCA Laboratories Princeton, New Jersey 08540	Unclassified
	2b. GROUP N/A

3. REPORT TITLE

Effects of Turbulence Instabilities on Laser Propagation

4. DESCRIPTIVE NOTES (Type of report and inclusive dates)

Quarterly Progress Report No. 4, 9 March 1972 - 8 June 1972

5. AUTHOR(S) (First name, middle initial, last name)

David A. de Wolf

6. REPORT DATE	7a. TOTAL NO. OF PAGES	7b. NO. OF REFS
July 1972	53	32

8a. CONTRACT OR GRANT NO.	9a. ORIGINATOR'S REPORT NUMBER(S)
F30602-71-C-0356	
b. PROJECT NO. ARPA 1279	PRRL-72-CR-25
c. Program Code IE-20	9b. OTHER REPORT NO(S) (Any other numbers that may be assigned this report) RADC TR-72-204
d.	

10. DISTRIBUTION STATEMENT

Approved for public release; distribution unlimited

11. SUPPLEMENTARY NOTES	12. SPONSORING MILITARY ACTIVITY
Monitored by: Lt. Darryl P. Greenwood (315) 330-3443: RADC (OCSE) GAFB, NY 13440	Defense Advanced Research Project Agency 1400 Wilson Blvd., Arlington, Va. 22209

13. ABSTRACT

This report consists of two parts. The first is a review and discussion of the contents of the three Quarterly Reports under the contract effort terminating on 8 June 1972. This discussion updates that work by comparing it with recent other work and new data. The basic results deal with the fluctuating properties of the focal area of a focused laser beam in turbulent air, viz.,

1. The average focal area for horizontal propagation.
2. An extension of (1) to slant-path geometry.
3. The power spectrum of the focal-spot radius.

The second part, self-contained, is a new theory of plane-wave irradiance scintillation. It contains the prediction that the log-amplitude variance is proportional to $L^{-1/2} (C_n^2)^{-1/6}$ in the saturation regime. The theory is an extension of the work presented recently in a Special Report under the present contract effort.

DD FORM 1 NOV 68 1473

Unclassified
Security Classification

14. KEY WORDS	LINK A		LINK B		LINK C	
	ROLE	WT	ROLE	WT	ROLE	WT
Wave Propagation Turbulent atmosphere, air Laser beam, focused Optics, atmospheric Irradiance fluctuations						

iia

EFFECTS OF TURBULENCE INSTABILITIES ON LASER PROPAGATION

DAVID A. de WOLF

CONTRACTOR: RCA LABORATORIES
CONTRACT NUMBER: F30602-71-C-0356
EFFECTIVE DATE OF CONTRACT: 9 JUNE 1971
CONTRACT EXPIRATION DATE: 8 JUNE 1972
AMOUNT OF CONTRACT: $49,990.00
PROGRAM CODE NUMBER: 1E20

INVESTIGATOR: DR. DAVID A. de WOLF
PHONE: 609 452-2700 EXT. 3023

PROJECT ENGINEER: LT. DARRYL P. GREENWOOD
PHONE: 315 330-3443

This research was supported by the Defense Advanced Research Projects Agency of the Department of Defense and was monitored by Lt. Darryl P. Greenwood, RADC(OCSE), GAFB, N.Y. 13440 under contract F30602-71-C-0356.

11h

FOREWORD

This Final Report was prepared by RCA Laboratories, Princeton, New Jersey under Contract No. F30602-71-C-0356. It describes work performed from 9 June 1971 to 8 June 1972 in the Communications Research Laboratory, Dr. K. H. Powers, Director. The principal investigator and project engineer is Dr. D. A. deWolf.

The report was submitted by the author on 7 July 1972. Submission of this report does not constitute Air Force approval of the report's findings or conclusions. It is submitted only for the exchange and stimulation of ideas.

The Air Force Program Monitor is Lt. Darryl P. Greenwood.

PUBLICATION REVIEW

This technical report has been reviewed and is approved.

Darryl P. Greenwood

RADC Project Engineer

SUMMARY AND ABSTRACT

This report consists of two parts. The first is a review and discussion of the contents of the three Quarterly Reports under the contract effort terminating on 8 June 1972. This discussion updates that work by comparing it with recent other work and new data. The basic results deal with the fluctuating properties of the focal area of a focused laser beam in turbulent air, viz.,

1. The average focal area for horizontal propagation.
2. An extension of (1) to slant-path geometry.
3. The power spectrum of the focal-spot radius.

The second part, self-contained, is a new theory of plane-wave irradiance scintillation. It contains the prediction that the log-amplitude variance is proportional to $L^{-1/2} (C_n^2)^{-1/6}$ in the saturation regime. The theory is an extension of the work presented recently in a Special Report under the present contract effort.

TABLE OF CONTENTS

LIST OF ILLUSTRATIONS

PART I

REVIEW AND DISCUSSION OF RESULTS

The results obtained and reported in [1] through [4] will be reviewed briefly, and discussed in context with the most recent developments elsewhere.

A. BROADENING OF A FOCUSED BEAM IN TURBULENT AIR

The focal spot of a focused laser beam scintillates because atmospheric turbulence causes irregularly varying undulations in the rays leaving the optical aperture and propagating to the focus (diffraction limited to an area characterized by a typical radial length $\sim r_{Lo} = kL/r_o$ where r_o is the aperture radius). Three specific calculations pertinent to this effect have been given.

1. The average area of the focal spot for horizontal propagation, i.e. uniform C_n^2.

2. An extension of (1) for slant-path propagation, using the altitude-dependent model of $C_n^2(z)$ summarized by Wyngaard, et al[5].

3. The power spectrum of the focal-spot radius.

The method of computing (1) requires some comment. A laser beam is a combination of modes in which a lowest-order mode usually dominates[6]. The ensuing expression for its electric field is too cumbersome for analytic work and consequently an approximate approach due to Schmeltzer[7] is

followed. It yields a result for the irradiance[1] that contains errors of $O(L/kr_o^2)$. At optical frequencies and for apertures of the order of 1-meter diameter the length $kr_o^2 \sim 10^3$ km and therefore this approximation is not serious for applications in which $L < 10$ km is envisioned. A second choice to be pondered is a suitable definition of focal-spot area. Several definitions have been proposed:

(a) The half-power radius r_L' defined so that the irradiance at $(\vec{r}_L', L)$ is related to that on the main axis at $(0,L)$ by $< I(\vec{r}_L', L) > = 0.5 < I(0,L) >$.

(b) A zero-th-moment radius r_L'',

$$(r_L'')^2 \equiv \int d^2\rho < I(\vec{\rho},L) > / < I(0,L) >$$

(c) A second-moment radius, r_L,

$$r_L^2 \equiv \int d^2\rho\, \rho^2 < I(\vec{\rho},L) > / \int d^2\rho < I(\vec{\rho},L) >$$

(d) An irradiance-squared definition, $r_L(I^2)$,

$$r_L^2(I) \equiv [\int d^2\rho < I(\vec{\rho},L) >]^2 / \int d^2\rho < I^2(\vec{\rho},L) >$$

Definitions (a) and (b) yield rather similar results which require a number of approximations in order to find some asymptotically valid analytical expressions. Definitions (c) and (d) can be modified in order to subtract out the diffraction-limited area $\sim r_{Lo}^2$. Definition (d) remains intractable analytically; however, Herrmann and Bradley[8] have used this

definition (without the averaging procedure) in a numerical solution of the parabolic wave equation. We prefer definition (c) because it yields a fundamental result that can be interpreted simply,[3]

$$r_L^2 = r_{Lo}^2 + 1.3\, L^3\, \kappa_m^{1/3}\, C_n^2, \tag{1}$$

where κ_m is the microscale wave number. This result has been compared to those obtained from (a) in [3], and it was concluded that the difference is not appreciable in spite of the fact (see Eq. (4) of [3]) that r_L' depends upon a somewhat different combination of powers of C_n^2, L, and k.

Recently [9] data on beam broadening have been reported. The accompanying analysis (and presentation) of these data correspond most closely with definition (a). Reasonable agreement between optical-frequency data and calculations exist, but the infra-red results are less in agreement. As well as we can infer at this time, beam-spread data was processed around a beam-wandering center. However, the analysis based on expressions (a) through (c) requires that no distinction be made between beam spread and wander. Specifically, the beam-wander variance $\langle \varphi^2 \rangle \sim C_n^2\, L\, b^{-1/3}$ where b is an effective beamwidth radius. The measured beam-spread parameter is $\langle \delta\varphi^2 \rangle = \langle \theta^2 \rangle - \langle \varphi^2 \rangle$ where $\langle \theta^2 \rangle$ is the angle associated with Equations (3), (4) of [3]. Thus

$$\begin{aligned} \langle \theta^2 \rangle &\sim C_n^2\, L\, \ell_o^{-1/3} && \text{for } 0.4\, k^2\, L\, \ell_o^{5/3}\, C_n^2 \gg 1 \\ &\sim C_n^{12/5}\, L^{6/5}\, k^{2/5} && \text{for } 0.4\, k^2\, L\, \ell_o^{5/3}\, C_n^2 \ll 1 \end{aligned} \tag{3}$$

We think the trouble may lie partly in the fact that $< \delta\varphi^2 >$ is processed as a measure of beam spread and then compared to a theoretical expression for $< \theta^2 >$ as in (3).

First consider the $\lambda = 0.6$-μm case. Let $\ell_o = 1$ cm, $C_n^2 \approx 10^{-13} m^{-2/3}$, $L = 1$ km. This makes $C_n^2 L$ correspond to the measured data. With these values, $0.4\, k^2 L\, \ell_o^{5/3} C_n^2 \approx 1$. Hence $< \theta^2 >$ is given by either of the two forms in (3); they are numerically the same. However, $b^{-1/3} \approx L_o^{-1/3} \approx 0.2\, \ell_o^{-1/3}$. Thus the <u>measured</u> quantity $< (\delta\varphi)^2 > \sim C_n^2 L\, (\ell_o^{-1/3} - b^{-1/3}) \sim 0.8\, C_n^2 L\, \ell_o^{-1/3} \sim 0.8 < \theta^2 >$ is interpreted analytically as $< \theta^2 >$. The error is at worst 20 percent. However, for $\lambda = 10.6$ μm, we find that $< \theta^2 >$ is now given by $C_n^{12/5} L^{6/5} k^{2/5}$, and is thus reduced at most by the factor $(0.6/10.6)^{2/5} \approx 0.3$. In that case $< \theta^2 > \approx 1.5 < \varphi^2 >$ and there is clearly an important difference between $< \delta\varphi^2 >$ and $< \theta^2 >$, namely $< \delta\varphi^2 > \approx 0.3 < \theta^2 >$. There might be an important discrepancy between measured and theoretical beam width at $\lambda = 10.6$ μm for this reason.

We have dealt with slant-path propagation in [3]. The basic problem is that the knowledge of $C_n^2(z)$ at altitudes z above several hundred meters is scant. We have simply extrapolated the $z^{-2/3}$ and $z^{-4/3}$ models of [5]. Instead of Eq. (1), we obtain for $r_L^2 - r_{Lo}^2 = r_{L_B}^2$,

$$r_{L_B}^2 = 3.9\, L^2 K_m^{1/3} \int_o^L ds\, (s/L)^2\, C_n^2(z) \qquad \text{downwards}$$

$$= 3.9\, L^2 K_m^{1/3} \int_o^L ds\, (1 - s/L)^2\, C_n^2(z) \qquad \text{upwards} \tag{2}$$

Greenwood[10] has evaluated these integrals in terms of hypergeometric functions. In [3] we present some asymptotic limits of $r_{L_B}^2$ as a function of the altitude Z of either the transmitter or receiver (one part of the link is always on the ground). The graphs of $r_{L_B}^2(Z)$ versus Z must be used with some caution when $Z > 500$ m, but they serve as a guideline.

The power-spectral analysis (3) has one important limitation; it is restricted to the angle of arrival of a ray. This appears to us to be correct for a <u>focused</u> beam as explained in Section IV.A of [3]. However, some question has now arisen with respect to the reinterpretation of the Gurvich, et al. data presented in Figure 10 of [11] which we discussed in [3]. It is possible that these data were gathered by an interferometric technique, and our theory is not applicable to an interferometer without modification. Nevertheless, the agreement of these data with the predictions in [3] appears to us to be excellent, so that possibly our reinterpretation remains valid.

B. IRRADIANCE SCINTILLATION OF A PLANE WAVE IN TURBULENT AIR

The second major part of our investigation deals with what is perhaps the most fundamental problem in the field: the amplitude fluctuations of a plane wave. As of June 1971, these fluctuations were known theoretically and experimentally to be governed by a log-normal probability distribution determined by a parameter $\sigma_\epsilon = 0.31\, k^{7/6} L^{11/6} C_n^2$ in the homogeneously turbulent (horizontal propagation) case. Under conditions in which σ_ϵ^2

exceeds unity it was observed that the log-amplitude variance saturates then decreases as σ_ϵ^2 increases. No satisfactory theoretical explanation has been given.

We have summarized extensively in a special report [4] what seems to us the most promising formalism for dealing with this problem: selective summation of terms in the infinite series of products of n-th Born terms in each moment of irradiance I. The most important facet of this report is the physical interpretation of the integrals which define the scattering processes; i.e. the physical interpretation of all the factors in each term. Furthermore, the report contains error bounds that appear more accurate than found elsewhere.

This work has led to an approximate solution in the saturation regime of the amplitude-fluctuation problem: the amplitude is still log-normal and its log-variance varies as $(\sigma_\epsilon^2)^{-1/6}$. The major break-through was to recognize the effect of ray-bending upon diffraction effects: a preliminary version of the new theory has been reported in [2]. The full theory--which includes a further elaboration of the work in [4]--is appended in this report in technical-report form.

C. ERRATA TO QUARTERLY REPORT NO. 3 (RADC-TR-72-119)[3]

In this section a few corrections to, and additional remarks about the results presented in the third Quarterly Report [3] will be added.

(i) The numerical coefficient in the denominator of r_{oc} in Eq. (10) should be $(1.3)^{+1/2} = 1.14$ (instead of 1.4).

(ii) Figures 2 and 3 give values of r_{oc} that are too high by a factor 10. To correct these and to make the results consistent with Eq. (10) and Figure 1, it is suggested that the values of the ordinates in Figures 2 and 3 be lowered by a factor 10.

(iii) The results of section II hold for air-to-ground propagation, whereas those of section III hold for ground-to-air propagation. Thus, Figure 5 is for slant-path, down situations and Figure 6 (the caption of which should refer to laser <u>targets</u>) for slant-path, up situations. All text in sections II and III should be modified in this sense. The origin of the original confusion is the <u>reciprocity</u> invoked in interpreting $< B(\vec{r},\vec{r}_1)B^*(\vec{r},\vec{r}_2) >$ in Eq. (A-3). The coordinate s in Eqs. (11) and (18) should have its zero at the <u>receiver</u> end because of reciprocity. The "dirty windshield" analogy is therefore not relevant.

(iv) An $\approx$ sign is needed in Eq. (36c).

(v) Table II is for $U_T = 0$ (not U_T-0).

(vi) Instead of Eq. (41b), we can obtain another approximation to $W_\theta(\omega)$ in the $\omega^{-2/3}$ region from Eq. (34) by setting q = 5/6 and $1+x \approx x$. It yields

$$W_\theta(\omega) \sim \frac{\pi^{1/2}\,\Gamma(1/3)}{(\Delta\omega)^{1/3}}\, M(1/6,1,-\Delta\omega^2/\omega_T^2)\cdot\omega^{-2/3}$$

where $M(={}_1F_1)$ is a Kummer function. This formula reduces to (36b) and (38b) for $\omega > \omega_T$; $\omega > \Delta\omega$.

REFERENCES

[1] D. A. de Wolf, "Effects of Turbulence Instabilities on Laser Propagation," RCA Laboratories, Quarterly Report to Rome Air Development Center, Griffiss AFB, New York, RADC-TR-71-249 (October 1971).

[2] D. A. de Wolf, "Effects of Turbulence Instabilities on Laser Propagation," RCA Laboratories, Quarterly Report to Rome Air Development Center, Griffiss AFB, New York, RADC-TR-72-32 (January 1972).

[3] D. A. de Wolf, "Effects of Turbulence Instabilities on Laser Propagation," RCA Laboratories, Quarterly Report to Rome Air Development Center, Griffiss AFB, New York, RADC-TR-72-119 (April 1972).

[4] D. A. de Wolf, "Strong Amplitude Fluctuations of Wave Fields Propagating Through Turbulent Media," RCA Laboratories, Technical Report to Rome Air Development Center, Griffiss AFB, New York, RADC-TR-72-51 (February 1972).

[5] J. C. Wyngaard, Y. Izumi, and S. A. Collins, Jr., J. Opt. Soc. Am. 61, 1646 (1971).

[6] H. Kogelnik and T. I. Lee, Appl. Optics 5, 1550 (1966).

[7] R. A. Schmeltzer, Quart. Appl. Math. 24, 339 (1967).

[8] J. Herrmann and L. C. Bradley, "Numerical Calculation of Light Propagation," Lincoln Laboratory, Laser Technology Program, Report LTP-10 (12 July 1971).

[9] J. A. Dowling, R. W. Harris, M. R. Kruer, and T. V. Blane, "Measurement of Wavelength Effects in the Propagation of Focused Laser Beams Through Atmospheric Turbulence," Paper WEB at 1972 Spring Meeting of O.S.A. (11-13 April 1972).

[10] D. P. Greenwood, "Slant Path Spherical-Wave Propagation," Paper WE16 at 1972 Spring Meeting of O.S.A. (11-13 April 1972).

[11] R. S. Lawrence and J. W. Strohbehn, Proc. IEEE 58, 1523 (1970).

PART II

STRONG IRRADIANCE FLUCTUATIONS IN TURBULENT AIR: PLANE WAVES*

By

D. A. de Wolf

RCA Laboratories

Princeton, New Jersey 08540

ABSTRACT

Analytical results are found for irradiance statistics of a plane wave propagating through uniformly turbulent air. They arise through a new error analysis of approximations made in selective summation of diagram contributions to the iterated moment equations (in integral form). The results are determined by three regimes of parameter $k^{7/6}L^{11/6}C_n^2$ determined by its location with respect to powers of the micro- and macroscale Fresnel numbers $(\kappa_m^2 L/k)^{-1/6} \sim 0.3$ and $(kL_o^2/L) \sim 10^4$ (the numerical values are for 0.6-μm radiation and a horizontal pathlength $L \sim 1$ km). The modified-Rytov result is found in the lowest regime. Irradiance I is log-normal in the intermediate (saturation) regime and the log-amplitude variance decays asymptotically as $(\kappa_m^{7/3}L^3C_n^2)^{-1/6}$. When $k^{7/6}L^{11/6}C_n^2$ far exceeds the macroscale Fresnel number kL_o^2/L, the irradiance tends to an exponential distribution (in agreement with previous results).

* This research was supported by the Advanced Research Projects Agency of the Department of Defense and was monitored by Rome Air Development Center under Contract No. F30602-71-C-0356.

This work deals with the statistics of the irradiance of an optical wave propagating through uniformly turbulent air. The fundamental statistics of even a plane wave in this medium have been predicted only for small and for extremely large values of the parameter $\sigma_\epsilon^2 \approx 0.31\, k^{7/6} L^{11/6} C_n^2$. This parameter, a function of pathlength L, wavenumber k, and refractive-index structure constant C_n^2, appears to be the one that governs the irradiance statistics for a plane wave. We will present new results for the hitherto unsolved intermediate region where σ_ϵ^2 exceeds unity but not necessarily by very much: the so-called saturation regime. Also, new error limits will be given that enable one to separate three regimes of statistical results for irradiance I, depending upon the magnitude of σ_ϵ^2 and the micro- and macroscale Fresnel numbers.

Tatarski [1] has pointed out that our previous result [2] yielding a constant-plus-Rayleigh distribution for I is incomplete due to omission of a class of diagram contributions. We have found this criticism to be correct, and consequently that result must be limited to the radiowave case [3] of large macroscale Fresnel numbers L/kL_o^2, in which case the partial summation suffices (but σ_ϵ^2 must then be replaced by $\alpha L \approx 0.2\, k^2 L L_o^{5/3} C_n^2$). Subsequently, we amended the optical case [4] to find an instantaneous ray solution with some of the experimentally observed characteristics of irradiance statistics. However, the solution only predicts the statistics of I globally, and the ray interpretation is questionable when $\sigma_\epsilon^2 > 1$.

The following pertinent developments have been reported in this journal: Sancer and Varvatsis [5] have presented an irradiance variance

vs σ_ϵ^2 curve that saturates, by solving an approximated equation. Brown [6] has voiced serious objections to their assumptions and approximations, and their results appear to be unconfirmed. Young [7] attributes saturation to beam spreading by atmospheric turbulence, but he does not attempt to give a full analysis. Molyneux [8] derives equations for the N-th moment of I, i.e., for $< I^N >$. He obtains the same result for $< I^2 >$ as in [3] and therefore Tatarski's criticism may hold here, too. A related development by Brown [9] also yields general moment equations. None of the above works allow predictions of the probability distribution of I. Furutsu [10] derives the moment equations once again by a method using characteristic functionals of the refractive index, and he finds that the logarithm of the irradiance follows a Rice distribution. This result has two peculiarities: (i) the irradiance variance goes to zero as the gaussian-beam field that is used as the free-space reference field approaches a plane wave, and (ii) the exponent of the mutual-coherence function is assumed to be a quadratic function of the separation distance of the correlated observation points. This prediction therefore does not appear to apply to a plane wave in turbulent air.

The situation in the USSR is somewhat more encouraging. Important work by Tatarski, Shishov, Klyatskin, and others prior to 1971, including numerical solutions [12] of the moment equations, is reviewed by Barabanenkov, et al. [11]. Since then, Gochelashvily and Shishov [13] have produced further analytical results: approximate solution of the $< I^2 >$ equations yields the Rytov approximation for small σ_ϵ^2, and - asymptotically - an exponential distribution of I at large distances.

Some preparation is needed to present the result of this paper. Consider error parameters:

$$\sigma_1^2 \equiv (\kappa_m^2 L/k)^{1/6}\sigma_\epsilon^2 \quad ,$$
$$\sigma_2^2 \equiv (L/kL_o^2)\sigma_1^2 \qquad (1)$$

where κ_m is the microscale wavenumber. For kilometer paths at optical frequencies, $\sigma_1^2 \approx 3\sigma_\epsilon^2$, and the numerical factor preceding σ_ϵ^2 varies slowly with L and k. The parametric dependence of σ_ϵ^2 upon L, k, and C_n^2 is obtained from the fact that $\sigma_\epsilon^2 = \langle \chi_1^2 \rangle$ where χ_1 is the real part of the complex phase ψ_1 of the Rytov approximation, which in turn is given by

$$\psi_1(L) = \frac{ik}{8\pi^2}\int_0^L dz \int d\underset{\sim}{\kappa}\,(\underset{\sim}{K},z)\exp[-iK^2(L-z)/2k] \quad , \qquad (2)$$

where $(2\pi)^{-2}d\underset{\sim}{\kappa}\,(\underset{\sim}{K},z)$ is a Fourier-Stieltjes increment of the permittivity deviation $\delta\underset{\sim}{\kappa}\,(\underset{\sim}{\rho},z)$ describing the Fourier analysis of this random process in any z = constant plane.

Our result is:

$$\begin{aligned} \langle I^N \rangle &= I_o^N \exp\{2N(N-1)\sigma_\epsilon^2[1+0(\sigma_1^2)^{5/6}]\} && \text{for } \sigma_1^2 \ll 1 \\ &= I_o^N \exp[2N(N-1)\sigma_\epsilon^2 \cdot 0(\sigma_1^2)^{-7/6}] && \text{for } \sigma_2^2 \ll 1 \ll \sigma_1^2 \\ &= N!\, I_o^N[1 + 0(\sigma_2^{1/3} e^{-\sigma_2})] && \text{for } 1 \ll \sigma_2^2 \end{aligned} \qquad (3)$$

The electric field $E = E_o \exp(\psi_1 - \sigma_\epsilon^2)$ for small values of σ_1^2. Thus the logarithm of the irradiance is normally distributed. For large values

of σ_2^2, the electric field is governed by a Rayleigh distribution of amplitude. There is an intermediate region $\sigma_2^2 \ll 1 \ll \sigma_1^2$ that yields a log-normal irradiance asymptotically as $\sigma_2^2 \to 0$ such that the log-amplitude variance is proportional to $(\sigma_\epsilon^2)^{-1/6}$. The "saturation" region form (for $1 \lesssim \sigma_1^2$) lies between the first two forms of (3) and it appears that I is log-normal and that the log-amplitude variance makes a transition from a linear dependence on σ_ϵ^2 to a dependence upon $(\sigma_\epsilon^2)^{-1/6}$ in agreement with experimental evidence.

The result is obtained by the method of selective summation of diagram contributions. The entire Born series for E is substituted into $< I^N >$ and the dominant contributions arising after a diagram renormalization of terms are summed. The error analysis is therefore a crucial aspect of the method. A geometrical-optics interpretation of the change-of-angle upon scattering allows one to estimate the error and to make very significant approximations.

I. THE BORN SERIES IN SMALL-ANGLE SCATTERING APPROXIMATION

A very brief derivation of the parabolic wave equation in the form most useful for selective-summation methods will be given because the source of the approximations needs to be specified carefully. The basic equation for a plane wave propagating from the origin plane z = 0 to the point of observation r = (0,0,L) is [4]:

$$B(\underset{\sim}{r}) = 1 + \frac{k^2}{4\pi^2} \int d^3 r_1 \int d\underset{\sim}{K}_1 (\underset{\sim}{K}_1, z_1) G(\underset{\sim}{r} - \underset{\sim}{r}_1) \exp(-i\underset{\sim}{K}_1 \cdot \underset{\sim}{\rho}_1) B(\underset{\sim}{r}_1) \qquad (4)$$

where coordinate $\underset{\sim}{r}_1 = (\underset{\sim}{\rho}_1, z_1)$, $d\&\ (\underset{\sim}{K}_1, z)$ is the two-dimensional Fourier-Stieltjes increment when the random variable $\delta\&\ (\underset{\sim}{r})$ is Fourier-analyzed in a z = constant plane, $B(\underset{\sim}{r})$ is the electric field $E(\underset{\sim}{r})$ divided by the equivalent free-space field $E_o(\underset{\sim}{r}) = \exp(ikz)$, and $G(\underset{\sim}{r}-\underset{\sim}{r}_1)$ is the Green's function multiplied by the factor $\{\exp[-ik(z-z_1)]\}$. The $d^2\rho_1$ integration in (4) can be performed. Let us write $B(\underset{\sim}{r}_1) = A(\underset{\sim}{r}_1)\exp[i\varphi(\underset{\sim}{r}_1)]$, with real functions A and φ. Then stationary-phase analysis [4] shows that the only region in the z_1 = const. plane of importance is the immediate vicinity of the stationary points $\underset{\sim}{\rho}_1$ that obey the equation

$$(\underset{\sim}{\rho}-\underset{\sim}{\rho}_1)/|\underset{\sim}{r}-\underset{\sim}{r}_1| = -\underset{\sim}{K}_1/k + k^{-1}\underset{\sim}{\nabla}_T\varphi(r_1) \tag{5}$$

where $\underset{\sim}{\nabla}_T$ is the transverse derivative, in this case at $\underset{\sim}{r}_1$.

However, the $d^2\rho_1$ integration is not carried out for (4), but for its iterated form $B = \sum_{n=o}^{\infty} B_n$, and it can be done without stationary-phase analysis to obtain,

$$B_n = \prod_{j=1}^{n} \frac{ik}{8\pi^2} \int_o^{\infty} dz_j \int d\&\ (\underset{\sim}{K}_j, z_j)$$

$$\times \prod_{m=1}^{n} (1-Q_m^2/k^2)^{1/2} \exp\{ik[(1-Q_m^2/k^2)^{1/2}|\Delta z_m| - \Delta z_m]\}\ , \tag{6}$$

$$\underset{\sim}{Q}_m = \sum_{j=m}^{n} \underset{\sim}{K}_j$$

where $\Delta z_m \equiv z_{m-1} - z_m$, $z_o = L$, and $\underset{\sim}{Q}_m$ is a shorthand notation that does not show the dependence on index n. If, however, a stationary-phase analysis is done on each $d^2\rho_m$ factor of B_n obtained from (4) by the n-th iteration, even though we did not use this analysis in deriving (6), we find that the only regions in the z_m = const. planes of importance

are the immediate vicinities of the stationary points $\underset{\sim}{\rho}_m$ that obey,

$$(\underset{\sim}{\rho}_{m-1}-\underset{\sim}{\rho}_m)/|\underset{\sim}{r}_{m-1}-\underset{\sim}{r}_m| = -\underset{\sim}{Q}_m/k \quad . \tag{7}$$

There is an important connection between (7) and (5) that we wish to exploit in this work. However, first we discuss two approximations always made in (6):

Approximation (i): We set $z_m < z_{m-1}$ for all z_m, i.e., backscatter contributions are ignored. The effect has been discussed before by many workers, e.g. in [11]. It can be understood by regarding the spectrum $\Phi(\underset{\sim}{K},k_z)$ of $\delta\tilde{\chi}(\underset{\sim}{\rho},z)$. The ratio of the variances of the $d\tilde{\chi}(\underset{\sim}{K}_j,z_j)$ factor in (6) when dz_j is integrated over a distance $-\Delta z$ and $+\Delta z$ is proportional to the ratio $\Phi(\underset{\sim}{K},2k)/\Phi(\underset{\sim}{K},0)$ where $2\pi L_o^{-1} < K < \kappa_m$. In optics $\Phi(\underset{\sim}{K},2k) \approx 0$ for all practical purposes and the dz_j integration over $-\Delta z$ is negligible.

Approximation (ii): Terms of $O(Q_m^2/k^2)$ are ignored compared to unity. When $n-m \ll 10$ one might estimate $Q_m^2/k^2 \lesssim \kappa_m^2/k^2 \ll 1$. Unfortunately, large-n terms are sometimes required, n-m can become large, and Q_m^2/k^2 may greatly exceed κ_m^2/k^2. Furthermore, there is a cumulative effect of errors due to dropping all Q_m^2/k^2 in $(1-Q_m^2/k^2)^{1/2}$ in (6).

A great aid in understanding the effect of terms of $O(Q_m^2/k^2)$ compared to unity in (6) is the geometrical interpretation of the vectors $\underset{\sim}{Q}_m/k$ given by (7). It states that $|\underset{\sim}{Q}_m/k|$ is the (sine of the) angle of the stationary-phase ray determined by the increments $d\tilde{\chi}(\underset{\sim}{K}_m,z_m)\cdots d\tilde{\chi}(K_n,z_n)$ for given z_m. Let us consider (7) for m=1, and simultaneously for all $n \geq 1$. Also, all $d\tilde{\chi}(\underset{\sim}{K}_j,z_j)$ are allowed to vary in all terms for $j > 1$

(i.e., the j = 1 increment is not varied). The total effect of $(\underset{\sim}{\rho}-\underset{\sim}{\rho}_1)/|\underset{\sim}{r}-\underset{\sim}{r}_1|$ of (7) in all these terms must be identical to that in (5). The total collection of all $\underset{\sim}{Q}_1/k$ (with correct sign preceding it), which we denote by $\{\underset{\sim}{Q}_1/k\}$ must then be identical in effect, as all $d\&\,(\underset{\sim}{K}_j,)z_j)$ are are varied, to the right-hand side of (5). Because the $\underset{\sim}{K}_1/k$ term subtracts out, we have,

$$\{\underset{\sim}{Q}_2/k\} = k^{-1}\underset{\sim}{\nabla}_T\varphi(r_1) \tag{8}$$

If we iterate (4) m-1 times, then find the stationary-phase equivalent of (5) for $\underset{\sim}{\rho}_{m-1}$ in the last term, and then apply the above comparison with (7) in similar fashion, we obtain

$$\{\underset{\sim}{Q}_{m+1}/k\} = k^{-1}\underset{\sim}{\nabla}_T\varphi(r_m) \tag{9}$$

in the understanding that $d\&\,(\underset{\sim}{K}_j,z_j)$ is varied for all $j > m$, and that all terms B_n with $n > m$ are considered simultaneously. This is an extremely valuable identification because the right-hand side of (9) can be identified with the angular deviation of a ray in a geometrical-optics medium:

$$k^{-1}\underset{\sim}{\nabla}_T\varphi(r_m) = d\underset{\sim}{\rho}(z_m)/dz_m \tag{10}$$

where the (for small angles quite permissible) approximation $d\underset{\sim}{\rho}/dr \approx d\underset{\sim}{\rho}/dz$ has been included. Note that we cannot replace any particular $\underset{\sim}{Q}_{m+1}/k$ by $d\underset{\sim}{\rho}/dz$ in (6). But we can estimate the effect of the $\{\underset{\sim}{Q}_{m+1}/k\}$ in (6) by regarding the behavior of $d\underset{\sim}{\rho}(z_m)/dz_m$ through application of (9) and (10). No matter how complicated $\varphi(\underset{\sim}{r}_m)$ actually is, the phase derivative is determined by the directions of the rays through the point $\underset{\sim}{r}_m$. Thus

$$\underset{\sim}{d\rho}(z_m)/dz_m = \frac{1}{2}\underset{\sim}{\nabla}_T \int_0^{z_m} dz\ \delta\varepsilon\ [\underset{\sim}{\rho}(z),z] \tag{11a}$$

after making the small-angle approximation of straightening rays. The right-hand side of (11a) is a statistical quantity that approaches a normal variable with zero mean and with variance,

$$< (d\underset{\sim}{\rho}_m/dz_m)^2 > \ \sim\ \kappa_m^{1/3} z_m C_n^2 \tag{11b}$$

in a turbulent medium with the usual modified Kolmogorov spectrum $<(\delta\varepsilon)^2>\Phi(K,0) \propto C_n^2 K^{-11/3}\exp(-K^2/\kappa_m^2)$. When $\kappa_m^{1/3} L C_n^2 \ll 1$, we can be sure that all Q_m^2/k^2 are small to this order because the statistical, nearly normal, variable $|d\underset{\sim}{\rho}/dz|$ will seldomly exceed several times its rms value determined by (11b). Thus, the approximation amounts to the neglect of diffusion effects: the cumulative scattering at large angles is ignored. In short, approximation (ii) is based on the statistical (geometrical-optics) estimate

$$Q_m^2/k^2 \lesssim O(\kappa_m^{1/3} L C_n^2)\ , \tag{12}$$

and when $\kappa_m^{1/3} L\, C_n^2 \ll 1$ we find that (6) reduces to,

$$B_n = \prod_{j=1}^{n} \frac{ik}{8\pi^2} \int_0^{z_j^{-1}} dz_j \int d\underset{\sim}{\kappa}\ (\underset{\sim}{K}_j, z_j) \cdot \prod_{m=1}^{n} \exp[-iQ_m^2 (z_{m-1} - z_m)/2k] \times [1+O(\kappa_m^{1/3} L\, C_n^2)] \tag{13}$$

There is an extra condition hidden in (13). When the factors $(1-Q_m^2/k^2)^{1/2}$ are expanded in a Taylor series in the exponential in (6), the leading terms are estimated from $ikz_m[(1-Q_m^2/k^2)^{1/2} - (1-Q_{m+1}^2/k^2)^{1/2}]$. The first one is given in (13), and the second one is $O(K_m^2 Q_{m+1}^2 L/k^3)$

and - in accordance with all sagittal approximations - it must be much less than π. Using (12), we find this error to be

$$O(K_m^2 Q_{m+1}^2 L/k^3) < O(L^2 \kappa_m^{1/3} k^{-1} L_o C_n^2)$$

hence $L^2 \kappa_m^{1/3} k^{-1} L_o C_n^2 \ll 1$ for validity of (13). However, because $L \ll k L_o^2$ we note that this condition is implied by $\kappa_m^{1/3} L C_n^2 \ll 1$, and therefore it need not be stressed.

Now we return to (13), which is equivalent to the parabolic equation [11], and rewrite it as

$$B_n = \prod_{j=o}^{n} \frac{ik}{8\pi^2} \int_o^{z_{j-1}} dz_j \int d\underset{\sim}{\kappa}\ (\underset{\sim}{K}_j, z_j) \times \{\prod_{m=1}^{n} \exp[-iK_m^2 (L-z_m)/2k] \exp[-i\underset{\sim}{K}_m \cdot \underset{\sim}{Q}_{m+1} (L-z_m)/k]\} \tag{14a}$$

The two exponential factors can be ignored in the high-frequency limit $k \to \infty$. As we have shown previously [3], and as Modesitt [14] has recently pointed out again, (14) can be summed to yield the WKB-phase integral in the form also known as the Moliere approximation. The Rytov approximation follows if only the second exponential factor for each m is ignored. The modified-Rytov approximation given in (3) for $\sigma_1^2 \ll 1$ follows by essentially ignoring this exponential factor in $< I^N >$ for $N > 1$ rather than in B. In fact, the study that follows is centered around the role of these exponential factors when (14) is substituted into $< I^N >$. Let us write (14a) formally in a short-hand notation:

$$B_n = \prod_{m=o}^{n} \int_o^{z_{m-1}} dz_m\ d\underset{\sim}{\kappa}\ (m) F_n(m) \tag{14b}$$

Let us first consider $< I^N >$ for N = 1. It consists of a sum of terms $< B_p B_q^* >$ in which p and q are summed from zero to infinity. Let us consider a particular term for which p + q = n. We write this term, using (14b), as

$$\int_0^L dz_1 \cdots \int_0^{z_{p-1}} dz_p \int_0^L dz_1' \cdots \int_0^{z'_{q-1}} dz_q' \quad d\&(1)F_p(1)\ldots d\&(q)F_q^*(q) \tag{15}$$

For given $z_1 \cdots z_p, z_1' \cdots z_q'$ we can rearrange the factors to become

$$\int_0^L dz_1'' \cdots \int_0^{z_{n-1}''} dz_n \quad d\&(1'')F_n(1'')\ldots d\&(n'')F_n(n'') \tag{16}$$

where $z_1'' \cdots z_n''$ is a permutation of $z_1 \cdots z_p, z_1' \cdots z_q'$ that leaves the ordering $z_{i-1} > z_i$ and $z_{j-1}' > z_j'$ unchanged. Likewise $F_n(i'')$ is one of the F_p or F_q^* factors depending upon which coordinate is permuted into z_i''. There are exactly n!/p!q! integrals of type (16) that constitute (15). A similar procedure can be carried out for N > 1 but obviously it is much more cumbersome to describe. The point is that (16) is now an ordered integral.

Two simplifications of the n-point integral in all terms (16) are possible regardless of the joint probability density of $d\&(1)\ldots d\&(n)$ provided the binary correlation length $\ell \ll L$ (the length ℓ is of the order of the macroscale L_o).

(i) The n-point correlation can be separated into $n!/2^{n/2}(n/2)!$ products of binary correlations $< d\&(i)d\&(j) >$. All products containing higher-order correlations are negligible by errors $O(L_o^2/L^2)$ to some power, and cumulatively by $O(k^2 L_o^2 \epsilon^2)$ where ϵ^2 is a short-hand

notation for the permittivity variance. The proof is given in [3] and more exhaustively by Brown [15].

(ii) Of the remaining products of binary correlations, only $<d\&(1'')\,d\&(2'')>\cdots<d\&(n-1'')\,d\&(n'')>$ is significant. The others contain at least two extra restrictions of intervals Δz to a distance $\sim L_o$ which introduces reduction factors of $O(L_o^2/L^2)$ per product and $O(k^2L_o^2\epsilon^2)$ cumulatively again. Furthermore there are some errors $O(Q_m^2/k^2)$ due to the F_n factors. These are negligible by virtue of (9)-(11).

In summary, the normalized electric field $B(=E/E_o)$ can be expressed as a sum of B_n over all integer n, which are given by (14). These are inserted into $<I^N> = I_o^N<(BB^*)^N>$ and the above properties (i) and (ii) are applied to the many ordered-integral terms which go into this N-th moment. The results are then restricted by errors $O(k^2L_o^2\epsilon^2)$ and $O(\kappa_m^{1/3}LC_n^2)$. Figure 1 is very useful for illustrating these. The cross-hatched areas are those where these errors are large. The other regions of this ϵ^2 (or C_n^2) vs L/L_o plot are useful for defining parameter regimes. Optical propagation appears to be restricted to regions I and III. The theoretical difficulties lie in the transition from III_w to III_s, because this is where σ_1^2 increases above unity. The other areas are more germane to radiowave propagation and they need not be discussed at present. Previous solutions for $<I^N>$ in [2] and [3] are restricted to regions I, II, and IV (when $N > 1$).

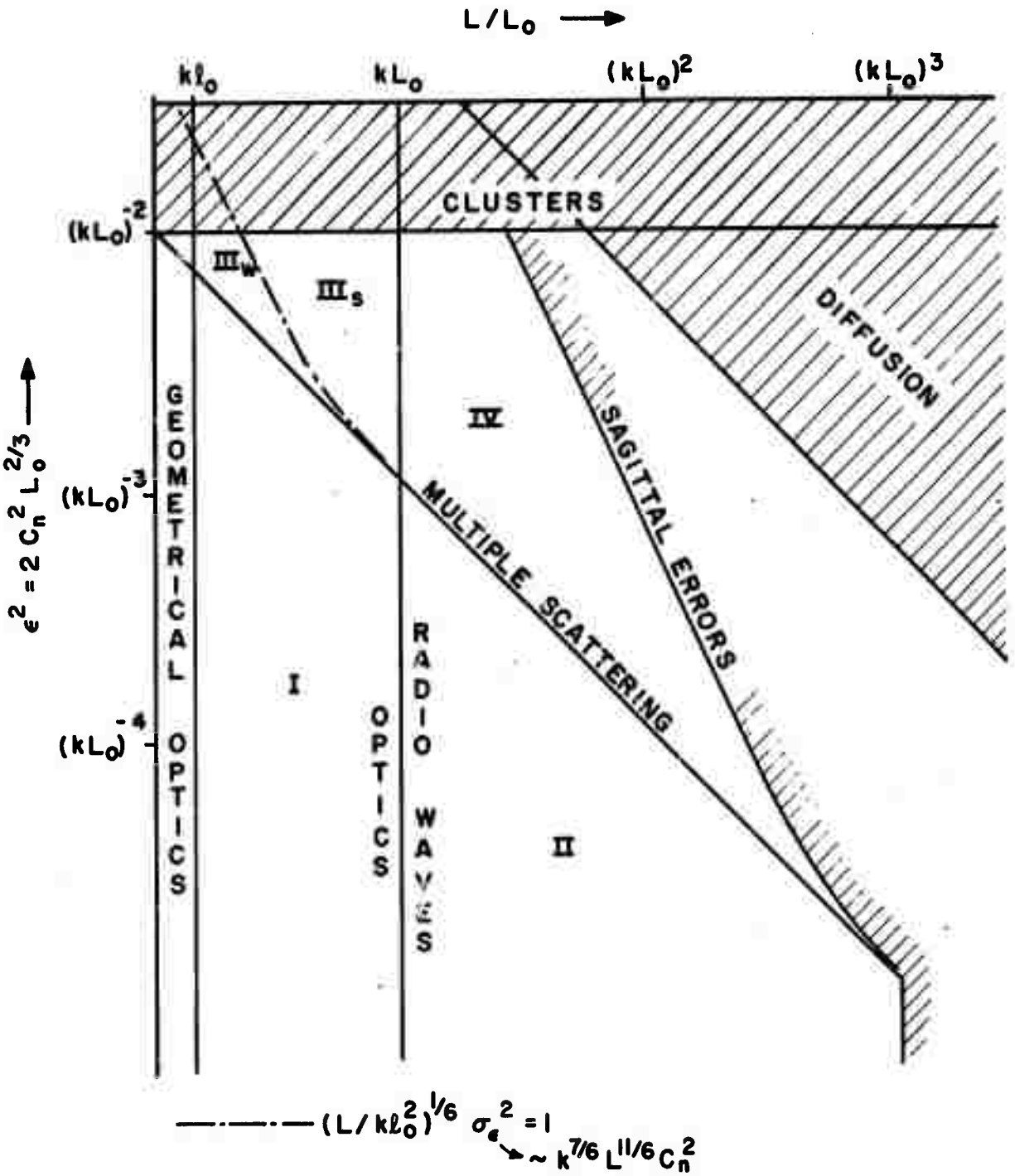

Figure 1. Parameter-region diagram for approximate solutions to the wave equation in turbulent air. Cross-hatched regions indicate breakdown of the parabolic equation and/or of important statistical assumptions.

II. THE MODIFIED-RYTOV APPROXIMATION

Let us consider $\langle I^2 \rangle$. It is determined by the sum over all integer n, m, p, q of $\langle B_n B_m^* B_p B_q^* \rangle$. Let $n+m+p+q = 2M$. The statistical simplification explained in connection with (15) allows one to represent $\langle I^2 \rangle$ by a sum of diagram contributions, each diagram corresponding not to n, m, p, and q, but to the half sum M. Each diagram consists of horizontal z-axes placed under each other, one for each B factor (dashed lines for B* axes) Each two-point correlation $\langle d\mathcal{E}(i)\, d\mathcal{E}(i+1) \rangle$ is represented by a "bead" on an axis, or by a "rung" between two axes, depending upon which B-factor the random increment $d\mathcal{E}$ (or perhaps its complex conjugate) is part of. Figure 2 gives some examples. It can be seen that $\langle I^2 \rangle$ is given by the sum of all topologically different diagrams with M features (M = 0, 1, $\cdots$). Note that an M = 2 diagram with a bead to the <u>left</u> of a rung is topologically different from one with a bead to the <u>right</u> of a rung. The diagram rules have been explained before [2,3].

Consider an M-feature diagram and keep features 2, 3, $\cdots$, M fixed. The <u>first</u> feature can then be one of the ten shown in Figure 3. We now utilize the following property in $\langle B_n B_m^* B_p B_q^* \rangle$ with (14),

$$\langle d\mathcal{E}(i)\, d\mathcal{E}(j) \rangle = 4\pi^2 \epsilon^2 \Phi_2(\underset{\sim}{K}_i, z_i - z_j) d^2K_i d^2K_j\, \delta_2(\underset{\sim}{K}_i \pm \underset{\sim}{K}_j), \qquad (17)$$

The minus sign in the (two-dimensional) Dirac delta factor holds if i belongs to a B and j to a B* factor, or vice-versa, and the plus sign in the two other cases. The function $\Phi_2(\underset{\sim}{K}, \Delta z)$ can be Fourier transformed with respect to Δz into the well-known three-dimensional spatial turbulence

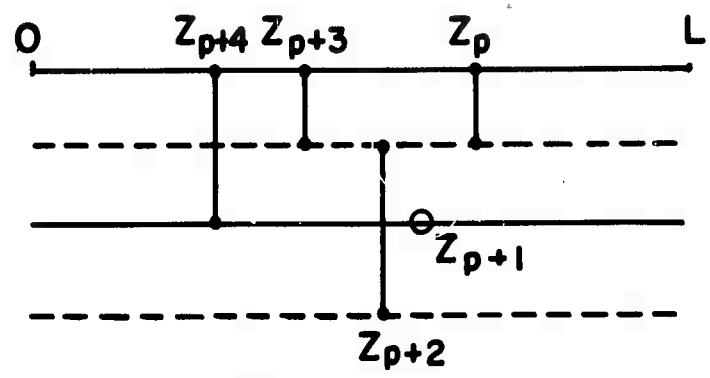

(a) A $B_n B_m^*$ RUNG AT Z_p

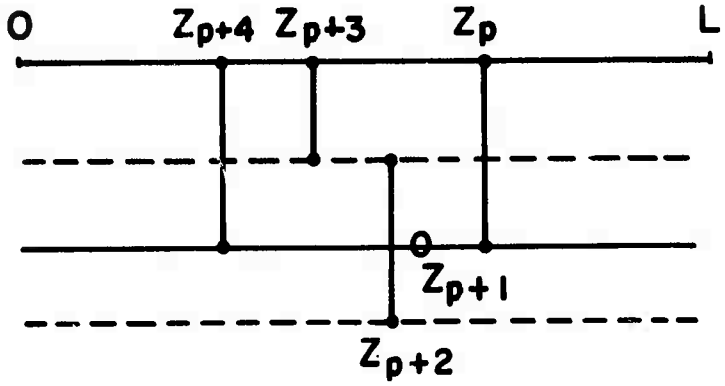

(b) A $B_n B_m$ RUNG AT Z_p

Figure 2. Two examples of diagrams symbolizing contributions to $<I^2>$.

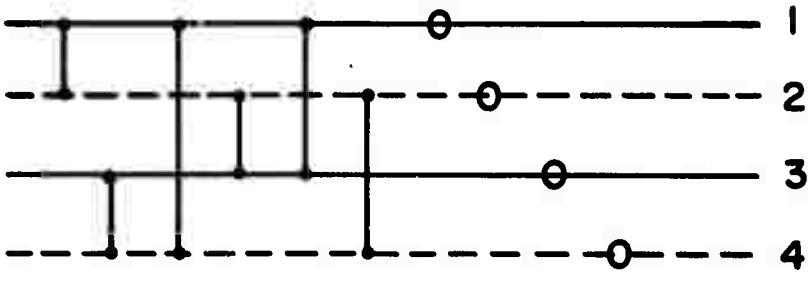

Figure 3. Ten possible locations of a feature of an $<I^2>$ diagram.

spectrum $\Phi(K,k_z)$. In the present work, the only form of the spectrum that will appear is $\Phi(K,0)$ which is written as $\Phi(K)$ for convenience. The first factor of the sum of ten M-feature diagrams thus obtained is

$$(k\epsilon/4\pi)^2 \int_0^L dz_1 \int d^2K_1 \Phi(K_1)$$

$$\times \{[C_1(12)+C_1(34)+C_1(14)+C_1(23)-2] - [C_1(13)+C_1(24)]C_1\} \qquad (18a)$$

$$C_1 \equiv \cos[K_1^2(L-z)/k]$$

$$C_1(ij) \equiv \cos[\underset{\sim}{K}_1 \cdot (\underset{\sim}{Q}_2^{(i)} - \underset{\sim}{Q}_2^{(j)})(L-z_1)/k]$$

The vectors $\underset{\sim}{Q}_2^{(i)}$ in the definitions of $C_1(ij)$ pertain to the sum of $\underset{\sim}{K}_p$-vectors, $p \geq 2$, connecting the i-th B axis of the diagram to all other axes. Note in particular that $\underset{\sim}{Q}_2^{(i)}$ and $\underset{\sim}{Q}_2^{(j)}$ are kept fixed for all ten diagrams generated by allowing the m = 1 feature to take all ten choices of Fig. 3. Note also that these ten diagrams have already incorporated some symmetry features with other sets of ten diagrams to yield only cosine factors in (18a). For example, the contribution $< B_m B_n^* B_p B_q^* >$ can be taken together with the $< B_n B_m^* B_q B_p^* >$ contribution. The second and other factors following (18a) cannot be written out in similar fashion because (18a) contains vectors $\underset{\sim}{K}_2, \cdots \underset{\sim}{K}_m$. If we were to change, say, the <u>second</u> feature (m = 2), then this would modify some of the $C_1(ij)$ factors in (18a). However, we can also take a particular M-diagram without allowing any of the features to be permuted, and then we obtain a contribution,

$$\int d^2K_1 \cdots \int d^2K_M \prod_{m=1}^{M} \frac{k^2\epsilon^2}{16\pi^2} \int_0^{z_{m-1}} dz_m \Phi(K_m) \times (-1)^{i+j-1} F_m(ij) \qquad (18b)$$

where $F_m(ij)$ stands for one of the cosine factors in $\{\cdots\}$ of (18a), but for any m, when $i \neq j$, and $F_m(ii) = 1/2$. All the bookkeeping difficulties lie in the $C_m(ij)$ factors. We will use both forms (18) in the following. Note finally that (18a) corresponds to the moment equation for $< I^2 >$ preferred by other workers.

The modified-Rytov approximation is obtained by setting all $C_m(ij) = 1$. Consider m = 1 first and set $C_1(ij) = 1$ in (18a), which then reduces to

$$\frac{k^2\epsilon^2}{4\pi} \int_o^L dz_1 \int_o^\infty dK_1 K_1 \Phi(K_1)\{1-\cos[K_1^2(L-z_1)/k]\} \ . \qquad (19)$$

This reduced form of (18a) is independent of vectors $\underset{\sim}{K}_2 \cdots \underset{\sim}{K}_m$. Therefore the m = 2 feature can be treated in exactly the same way as the m = 1 feature in (18a); after permutation of the second feature a common factor identical to (18a) results except that we have $C_2(ij)$ factors. Now we set $C_2(ij) = 1$ to obtain a form similar to (19). The product of all these factors for m = 1 to m = M must exhaust all possible M-feature diagrams. One need only sum from M = 0 to M = ∞ to obtain $< I^2 >$, i.e.

$$\begin{aligned} < I^2 > &= I_o^2 \sum_{m=o}^{\infty} \prod_{m=1}^{M} \frac{k^2\epsilon^2}{4\pi} \int_o^{z_{m-1}} dz_m \int_o^\infty dK_m K_m \Phi(K_m)(1-C_m) \\ &= I_o^2 \exp[\frac{k^2\epsilon^2}{4\pi} \int_o^L dz \int_o^\infty dK_1 K_1 \Phi(K_1)(1-C_1)] \qquad (20) \\ &= I_o^2 \exp(4\sigma_\epsilon^2) \ . \end{aligned}$$

The procedure is easily generalized for $< I^N >$ with N > 2. An expression similar to (18a) can be written down; the main difference is that $C_1(12) + \cdots + C_1(23)$ is replaced by a sum of N^2 terms corresponding to

$< BB^* >$ rungs, the numerical term -2 is replaced by -N, and $C_1(13)+C_1(24)$ is replaced by N(N-1) terms exhausting all $< BB >$ and $< B^*B^* >$ rungs. It need not be written down. The same procedure is easily observed to yield,

$$< I^N > = I_c{}^N \exp[2N(N-1)\sigma_\epsilon{}^2] \quad . \tag{21}$$

In this fashion, the first of Eqs. (3) is easily derived. The remaining analysis of this result is for the purpose of estimating the error induced by setting all $C_m(ij) = 1$. We shall do this systematically, first for m = 1 then for m = 2,3,$\cdots$, etc. It is preferable, however, to simplify (18a) first by means of an intermediate renormalization which simplifies the diagram bookkeeping.

RENORMALIZED BEADLESS DIAGRAMS

There is a contribution of a numerical term -2 in the { } factor in (18a) due to the four possible positions of beads in the first factor. It is therefore quite easy to renormalize the integrals by summing out the contribution of all beads, and the advantage of the new expressions is that the renormalized diagrams have rungs only. Let us start with any diagram without beads interpreted by means of (18b). Consider in this diagram any axis segment between two contiguous rungs. Now generate a new set of diagrams by placing zero, one, two, --- beads on this particular segment. The sum of the contributions from these new diagrams can be seen from (18b) to correspond to an extra factor

$$\exp\left[-\frac{k^2\epsilon^2}{16\pi}\int_0^\infty dK K\Phi(K)(z_{m-1}-z_m)\right] = \exp[-\alpha(z_{m-1}-z_m)]$$

in the contribution (18b). We can do the same thing for <u>every</u> axis segment of the original diagram. The result is,

(i) we have generated all possible diagrams with M rungs and any number of beads;

(ii) we have generated a factor $\exp(-\alpha L)$ for every horizontal axis, i.e., a factor $\exp(-4\alpha L)$ for every $< I^2 >$ renormalized diagrams. (The explicit form of αL is given in the introduction.)

Clearly there is nothing special about M, and the net result is that we can restrict ourselves to beadless diagrams. An M-rung renormalized diagram is interpreted as follows. The corollary of (18a) is

$$\exp(-4\alpha L)\cdot(k\epsilon/4\pi)^2 \int_0^L dz_1 \int d^2K_1 \Phi(K_1)$$
$$\times \{[C_1(12)+C_1(34)+C_1(14)+C_1(23)-C_1(13)-C_1(24)] \qquad (22)$$
$$+[C_1(13)+C_1(24)](1-C_1)\} ,$$

and the corollary of (18b) will not be written down here because it differs only by a factor $\exp(-4\alpha L)$. Note that we have reordered the terms somewhat in (22), aside from the renormalization. Steps (19)-(21) are easily repeated, using (22). The only difference is that $\{\cdots\}$ reduces to $2 + 2(1-C_1)$ which yields a factor $4\alpha L + 4\sigma_\epsilon^2$ at all places in (20) and (21) where previously only $4\sigma_\epsilon^2$ appeared. This cancels the factor $\exp(-4\alpha L)$. There is a definite advantage to the reordering in (22) which will become apparent in the error analysis. In order to investigate the effect of setting $C_1(ij) = 1$ in (22), we utilize (23a) as the prototype for analyzing any of the terms in the second row of (22),

and (23b) for the third row of (22).

$$(k\epsilon/4\pi)^2 \int_0^L dz \int d^2K\Phi(K)\cos[\underset{\sim}{K}\cdot\Delta\underset{\sim}{Q}(L-z)k] \tag{23a}$$

$$(k\epsilon/4\pi)^2 \int_0^L dz \int d^2K\Phi(K)\{1-\cos[K^2(L-z)/k]\}\cos[\underset{\sim}{K}\cdot\Delta\underset{\sim}{Q}(L-z)/k] \tag{23b}$$

Here, $\Delta\underset{\sim}{Q}$ is a short-hand notation for $\underset{\sim}{Q}_2^{(i)} - \underset{\sim}{Q}_2^{(j)}$. The error analysis is not affected if (L-z) in (23) is replaced by L, to obtain

$$(k^2\epsilon^2 L/8\pi) \int_0^\infty dK K\Phi(K)J_o(K\Delta QL/k) \tag{24a}$$

$$(k^2\epsilon^2 L/8\pi) \int_0^\infty dK K\Phi(K)J_o(K\Delta QL/k)\{1-(\kappa/K^2L)\sin(K^2L/k)\}\ , \tag{24b}$$

where J_o is a Bessel function. From here on, the Kolmogorov spectrum [16] is used, with the von Karman modification for wavenumbers $K < L_o^{-1}$:

$$\Phi(K) \approx 15.7L_o^3(1+K^2L_o^2)^{-11/6}\exp(-K^2/\kappa_m^2) \tag{25}$$

The numerical factor in (25) differs from that used by Tatarski [16] due to a different Fourier-transform normalization. Insertion of (25) into (24) yields forms which serve as the basis for error analysis:

$$(15.7/4\pi)k^2\epsilon^2 LL_o[\sigma_2^{5/6}K_{5/6}(\sigma_2)/2^{11/6}\Gamma(11/6)]\ , \tag{26a}$$

with $\sigma_2 \equiv \Delta QL/kL_o$,

$$4\sigma_\epsilon^2 b_x(\sigma_1) \text{ with } \sigma_1 = \Delta Q(L/k)^{1/2}. \tag{26b}$$

Here, $K_{5/6}(\sigma_2)$ is a modified Bessel function, $\Gamma(11/6)$ is a gamma function, and $b_x(\sigma_1)$ is related to a confluent hypergeometric function, specifically by Eq. (47.33) of [16]. Only the following two limiting

forms of this function are required in this work:

$$b_x(\sigma_1) = 1 - 2.36(\sigma_1^2)^{5/6} \text{ as } \sigma_1 \to 0$$
$$= -0.0242(\sigma_1^2/4)^{-7/6} \text{ as } \sigma_1 \to \infty \tag{27}$$

There is a small detail in the $\sigma_1 \to 0$ form regarding the magnitude of σ_1^2 with respect to the inverse microscale Fresnel number $k\ell_o^2/L$ that is of no importance here (it is assumed that σ_1^2 does not decrease below this number). With (26) it is easily seen for small $\Delta Q/k$ that (26) reduces to,

$$4\alpha L[1 + 0(\sigma_2^2)^{5/6}] \tag{28a}$$

$$4\sigma\epsilon^2[1 + 0(\sigma_1^2)^{5/6}] \tag{28b}$$

A factor 2 has been multiplied into (26) and (28) to make (24) correspond to the sum of terms in (22). Furthermore, the definitions imply that $\sigma_2^2 \ll \sigma_1^2$ so that it suffices to require $\sigma_1^2 \ll 1$ in (28b) in order that the modified-Rytov expressions (20) and (21) follow.

With the development of (9)-(11), it then follows that σ_1^2 can be identified with the parameter of Eq. (1). There is one difference. In considering (22) for $C_1(ij)$, it is necessary to consider simultaneously <u>all</u> diagrams with $M \geq 1$. In that case $\underset{\sim}{Q}_2/k$ can be identified again with $k^{-1}\underset{\sim}{\nabla}_T\varphi(r_1)$, and $\Delta\underset{\sim}{Q}_2/k$ is then certainly less than $2k^{-1}\underset{\sim}{\nabla}_T\varphi(r_1)$; it can even be zero if the two runged axes to which $\Delta\underset{\sim}{Q}_2$ belong form an unconnected subdiagram. However, in the worst case, we can replace $(\Delta Q/k)^2$ by $4L\kappa_m^{1/3}C_n^2$ (ignoring a factor of order unity) and thus convert the above defined parameters σ_1^2 and σ_2^2 to,

$$\sigma_1^2 \leftrightarrow kL^2 K_m^{1/3} C_n^2 = (K_m^2 L/k)^{1/6}(k^{7/6} L^{11/6} C_n^2)$$
$$\sigma_2^2 \leftrightarrow (L/kL_o^2)\sigma_1^2 \quad . \tag{29}$$

III. THE SATURATION REGIME: $1 < k^{7/6} L^{11/6} C_n^2 \ll kL_o^2/L$

The results of the previous section indicate that the log-amplitude (or log-irradiance) variance is a linear function of the parameter $\sigma_\epsilon^2 \sim k^{7/6} L^{11/6} C_n^2$. All measurements to date show a variation from this behavior when $\sigma_\epsilon^2 > 1$; a saturation effect occurs in the sense that the variance attains a maximum value close to $\sigma_\epsilon^2 = 1$. We shall define a saturation regime by the inequality $1 < \sigma_\epsilon^2 \ll kL_o^2/L$, and it corresponds reasonably well to the slightly sharper inequality $\sigma_2^2 \ll 1 \ll \sigma_1^2$ whenever the identification (29) is utilized.

Clearly $\sigma_\epsilon^2 \ll kL_o^2/L$ does imply that $\Delta Q/k$ in the first set of terms of {---} in (22) is small enough to set $C_1(ij) = 1 + O(\sigma_2^2)^{5/6}$ for the same reasons as set forth in Eqs. (23)-(28). Consequently, (22) reduces to,

$$\exp(-4\alpha L)\cdot[(k\epsilon/4\pi)^2 \int_o^L dz_1 \int d^2K_1 \Phi(K_1)\{2 + [C_1(13)+C_1(24)][1-C_1]\}] \tag{30}$$

Through an obvious symmetry property that maps every diagram of $< BB^*BB^* >$ into one of $< B^*BB^*B >$, and vice-versa, $C_1(24)$ may be replaced by $C_1(13)$. The filter factor {---} in (39) reduces to $2\{1 + [C_1(13)][1-C_1]\}$. A rough estimate, similar to that of Eqs. (23)-(28), yields something like $\exp(-4\alpha L)\cdot[4\alpha L + 4\sigma_\epsilon^2 b_x(\sigma_1^2)]$ for (30). It

shows, using (27), that the term proportional to $4\sigma_\epsilon^2$ is modified drastically as σ_1^2 increases above unity. Therefore (28b) is not valid, and (20) does not follow in this case.

The following approximation is the basis for a saturation-regime result: Replace all $\underset{\sim}{Q}_{m+1}^{(i)}/k$ by the function $\underset{\sim}{\rho}_i(z_m)$ to be defined later. The index i pertains to the B factor in question. Then replace $C_m(13)$ by an average $<C_m(13)>$. All M factors are now separable and we can reduce $<I^2>$ to an exponential form in the same way that (20) was derived from its defining series:

$$<I^2> = I_o^2 \exp\{2(k\epsilon/4\pi)^2 \int_o^L dz_1 \int d^2K_1 \Phi(K_1)(1-C_1) \times <\cos[K\cdot\Delta\rho(z)]> + O(\sigma_2^2)^{5/6}\} \tag{31}$$

It is reasonable because of the following arguments: The rough estimate of (30) indicates that the M-th order term of $<I^2>$ is of order $(4\alpha L)^M/M!$ if effects of $O(\sigma_\epsilon^2)$ compared to αL are ignored. Terms with $M \ll 4\alpha L$ ($4\alpha L$ is a very large number compared to unity) are unimportant and consequently $\underset{\sim}{Q}_2$ is a sum of a large number of vectors $\underset{\sim}{K}_j$. Furthermore, $\underset{\sim}{Q}_2^{(1)} - \underset{\sim}{Q}_2^{(3)}$ contains a sum of M-1 non-cancelling K_j vectors (some of these occur with a factor 2) because the binary-correlation property (17) implies

$$\underset{\sim}{Q}_m^{(1)} - \underset{\sim}{Q}_m^{(2)} + \underset{\sim}{Q}_m^{(3)} - \underset{\sim}{Q}_m^{(4)} = 0 \tag{32}$$

for all m. Consider the $C_1(13)$ factor in (30). It is a function of

of $\Phi(K_2)d^2K_2 \cdots \Phi(K_M)d^2K_M$ with the other M-1 filter factors. Because $2-2C_m(13)(1-C_m) \approx 2$ in the integrand it follows that the main contribution of $C_1(13)(1-C_1)$ is found by setting the other M-1 filter factors equal to 2 [see the discussion immediately following (30)]. Consequently $C_1(13)$ is a function of $\underset{\sim}{Q}_2^{(1)} - \underset{\sim}{Q}_2^{(3)}$ which is a sum of all $\underset{\sim}{K}_j$ vectors of the remaining integrand $\Phi(K_2)d^2K_2 \cdots \Phi(K_m)d^2K_m$. There is complete analogy to a two-dimensional random-walk problem where $\underset{\sim}{K}_j$ is a random phasor and $\Phi(K_j)$ its probability density. Therefore $\underset{\sim}{Q}_2^{(1)} - \underset{\sim}{Q}_2^{(2)}$ tends to a Gaussian random variable because M is large, and with zero mean. We replace it by a quantity with the same statistical properties and then replace $C_1(13)$ by $\langle C_1(13) \rangle$. This Gaussian quantity will be named $\underset{\sim}{\Delta\rho}(z)$ at present and it will be identified in the Appendix with ray coordinates. However, at present it need not be discussed further. After having made the substitution for $\underset{\sim}{Q}_2/k$, we now consider the M = 2 factor analogous to (30), and repeat the very same argument for $C_2(13)$ - which involves only the $\Phi(K_3)d^2K_3 \cdots \Phi(K_m)d^2K_m$ factors. As $m \to M$ it appears incorrect to continue this procedure because the number M-1-m of $\underset{\sim}{K}_j$ vectors in $\underset{\sim}{Q}_{m+1}^{(1)} - \underset{\sim}{Q}_{m+1}^{(3)}$ becomes small. Nevertheless, the error in so doing is small because the M-th term of $\langle I^2 \rangle$ is considered together with many subsequent higher-order terms in which z_m is not one of the last z coordinates.

A straight-forward extension of the procedure to $\langle I^N \rangle$ yields

$$\langle I^N \rangle = I_o{}^N \exp\{2N(N-1)(k\epsilon/4\pi)^2 \int_o^L dz_1 \int d^2K_1 \Phi(K_1)(1-C_1) \times \langle \cos[K_1 \cdot \Delta\rho(z_1)] \rangle + N0(\sigma_2{}^2)^{5/6}\} \tag{33}$$

The important point is not that $\underset{\sim}{Q}_{m+1}/k$ has been replaced by $\underset{\sim}{\rho}(z)$ but that $C_m(13)$ has been replaced by an average $< C_m(13) >$ which is not a function of $\underset{\sim}{K}_{m+1}, \cdots \underset{\sim}{K}_M$. If we may ignore $O(\sigma_2^2)$ we then note that we have shown in (33) that the irradiance is also log-normal in the saturation regime.

The $O(\sigma_2^2)$ effects become negligible as the Fresnel number L/kL_o^2 goes to zero. Consider this limit for the sake of clarifying (33). As $\sigma_\epsilon^2 \to \infty$ (or $\sigma_1^2 \to \infty$) the irradiance I reduces to I_o because the error term in (33) is $O(\sigma_\epsilon^2)^{-1/6}$. The only way to allow $\sigma_\epsilon^2 \to \infty$ consistent with $L/kL_o^2 \to 0$ and with the diffusion condition (12), namely $K_m^{1/3} L C_n^2 \ll 1$, is to allow $k \to \infty$. So this transition is essentially to a high-frequency limit in which case it is not surprising that $I \to I_o$ [17].

However, our interest is in the case that k = const. and that C_n^2 and/or L increase. Let us take L ~ 1 km and allow C_n^2 to increase since this is in accord with the experimental situation. The Fresnel number $L/kL_o^2 \sim 10^4$ at optical frequencies. Thus $\sigma_2^2 \sim 10^{-4}\sigma_1^2$ and the $O(\sigma_2^2)^{5/6}$ terms can be kept very small in (34) compared to the $O(\sigma_\epsilon^2)^{-1/6}$ terms for $\sigma_1^2 > 10$.

Finally, in the Appendix we work out an estimate of (33). It yields,

$$< I^N > = I_o^N \exp[2N(N-1)\sigma_\epsilon^2 \cdot O(\sigma_1^2)^{-7/6}] \quad . \tag{34}$$

The last result indicates that the log-amplitude variance decreases asymptotically as $\sigma_\epsilon^2 \cdot O(\sigma_1^2)^{-7/6} \sim O(\sigma_\epsilon^2)^{-1/6}$. We discuss this further

in section V. The decrease with increasing σ_ϵ^2 cannot continue indefinitely because ultimately σ_2^2 exceeds unity and expression (30) is no longer valid. An asymptotic solution for the case that $\sigma_2^2 \to \infty$ will be given in the next section.

IV. THE RAYLEIGH REGIME: $k^{7/6}L^{11/6}C_n^2 \gg kL_o^2/L$

Expressions (24) or, equivalently, (26) have to be handled quite differently when $\sigma_2^2 \gg 1$. They then reduce to

$$4\alpha L[\pi^{1/2}/2^{7/3}\Gamma(5/6)]\cdot\sigma_2^{1/3}\exp(-\sigma_2) \tag{35a}$$

$$4\sigma_\epsilon^2\cdot 0(\sigma_1^2)^{-7/6} \tag{35b}$$

Both of these forms vanish as $\sigma_2^2 \to \infty$ and therefore we can no longer utilize the grouping of terms in (22). Previously, the grouping of terms in the second line of (22) yielded a factor 2, regardless of whether $\Delta Q = 0$ or $\Delta Q \neq 0$ in any of the $C_1(ij)$. Now it does make a difference; for $\Delta Q \neq 0$, $C_1(ij)$ reduces to a vanishingly small term as $\sigma_2 \to \infty$, in contrast to the case $\Delta Q = 0$ which yields $C_1(ij) = 1$. In this case, we utilize the corollary of (18b) which differs from (18b) by an exponential factor, and by omission of $i = j$ factors. Evidently, the main contribution now comes from a subclass of diagrams: those for which <u>all</u> $C_m(ij) = 1$, i.e. for which all $\Delta Q = 0$. Inspection of the renormalized beadless diagrams in conjunction with the property (32) shows that this subclass of diagrams has the following properties:

(i) There are no $< 13 >$ nor $< 24 >$ rungs (the notation $< 13 >$ indicates correlation between the first and the third horizontal axes). In general, there are no $< BB >$ nor $< B^*B^* >$ rungs.

(ii) Any B axis is connected by rungs to only one B* axis, and vice versa. That is to say, all diagrams can be factored into products of $< BB^* >$ diagrams.

Instead of (22) and similar factors for m = 2,---,M as the contribution of a diagram with M rungs to $< I^2 >$, we have in general for $< I^N >$ according to the above procedure,

$$\exp(-2N\alpha L)\cdot\prod_{m=1}^{M}\frac{k^2\epsilon^2}{16\pi^2}\int_0^{z_{m-1}} dz_m\int d^2K_m\,\Phi(K_m)C_m(ij)$$
$$= \exp(-2N\alpha L)\cdot(2\alpha L)^M/M! \qquad (36)$$

Let us try to add up (36) for all M-rung diagrams where n pairs of B and B* axes have no rungs. We may not have any mixing, i.e., we cannot have two rungs connecting <u>one</u> B to <u>two</u> B* axes, or vice versa, otherwise at least one $C_m(ij) \neq 1$. For <u>one</u> choice of n pairs of conjugate B and B* axes there are (N-n)! ways of pairing the remaining N-n pairs of B and B* axes two by two. Let us assume for one choice of pairing that there are $m_1, m_2, \text{---} m_{N-n}$ rungs on the N-n pairs we have chosen. Obviously $m_1 + \text{---} + m_{N-n} = M$. Then we obtain

$$(N-n)!\; e^{-2N\alpha L} \sum_{m_1=1}^{\infty} \cdots \sum_{m_{N-n}=1}^{\infty} \frac{M!}{m_1! \cdots m_{N-n}!} \cdot e^{-M\alpha L} =$$

$$= (N-n)!\; e^{2N\alpha L}(1-e^{-2\alpha L})^{N-n} \quad , \tag{37}$$

for all M-rung diagrams that leave a single choice of n pairs of B,B* axes unconnected to each other by rungs. We need one more numerical factor in (37) before summing over n from n = 0 to n = N, namely the number of ways that we can choose n pairs B and B* from N pairs B and B*. This number is easily seen to be

$$\frac{N^2(N-1)^2 \cdots (N-n+1)^2}{1^2 2^2 \cdots n^2} = \frac{(N!)^2}{(n!)^2[(N-n)!]^2} \tag{38}$$

Thus, we obtain $\langle I^N \rangle / \langle I \rangle^N$ by summing the product of (37) with (38) over n from n = 0 to n = N:

$$\langle I^N \rangle = \langle I \rangle^N \sum_{n=0}^{N} \frac{(N!)^2}{(n!)^2(N-n)!} e^{-2n\alpha L} (1-e^{-2\alpha L})^{N-n} \tag{39}$$

The meaning of (39) for small and intermediate αL has been worked out in [2] and [3], but in the present case $\alpha L \gg 1$ and we retain only the n = 0 term in (39) to obtain,

$$\langle I^N \rangle = N!\; I_o{}^N [1 + O(\sigma_2{}^{1/3} e^{-\sigma_2})] \tag{40}$$

This result is the Rayleigh limit: a special case of a result found earlier [2] for region IV of Fig. 1 where αL had not greatly exceeded unity. It states that as $\sigma_2 \to \infty$, the irradiance approaches an exponential distribution (i.e., the amplitude becomes Rayleigh-distributed).

V. COMMENTS ON THE IRRADIANCE-VARIANCE SATURATION

The results (3) - or more fully (21), (28), (29), (34), and (40) - allow us to reconsider the irradiance-variance saturation. It seems somewhat easier to consider the log-amplitude $\chi = \frac{1}{2} \ln I$ and to plot $\langle \chi^2 \rangle$ as a function of σ_ϵ^2. The results indicate:

(i) $\langle \chi^2 \rangle = \sigma_\epsilon^2$ for values of σ_ϵ^2 much less than $(\kappa_m^2 L/k)^{-1/6}$, a number of order unity.

(ii) $\langle \chi^2 \rangle \propto \sigma_\epsilon^2 \cdot (\sigma_1^2)^{-7/6} \propto (\sigma_\epsilon^2)^{-1/6}$ for intermediate values $(\kappa_m^2 L/k)^{-1/6} \ll \sigma_\epsilon^2 \ll kL_o^2/L$. The log-amplitude variance changes from linear growth to a decrease as $(\sigma_\epsilon^2)^{-1/6}$ as σ_ϵ^2 grows beyond a number of order unity. This trend appears to agree well with experimental observation.

(iii) $\langle \chi^2 \rangle$ should level off asymptotically at the level $\pi^2/24 \approx 0.41$ when the Rayleigh limit is reached, i.e., when $\sigma_\epsilon^2 \gg kL_o^2/L$. It depends on the magnitude of kL_o^2/L whether $\langle \chi^2 \rangle$ has dropped below $\pi^2/24$ before leveling off or not.

Experimental data now exists with which to check these aspects of the theory. Mevers, et al. [18] have found a decrease with $(\sigma_\epsilon^2)^{-0.17}$ in region (ii), in good agreement with our result. The newer data of Kleen and Ochs [19] as well as the older data of Gracheva [20] exhibit a trend of this type (although no analytical expression for their data is given and although their data exhibit appreciable spread). Furthermore,

$<\chi^2>$ appears to drop below the ultimate level of $\pi^2/24$ (presumably because $kL_o^2/L \sim 10^4$ is so large a number).

Figure 4 gives a sketch of a saturation curve satisfying the above predictions. The dip below the Rayleigh limit $\pi^2/24$ has been shown in

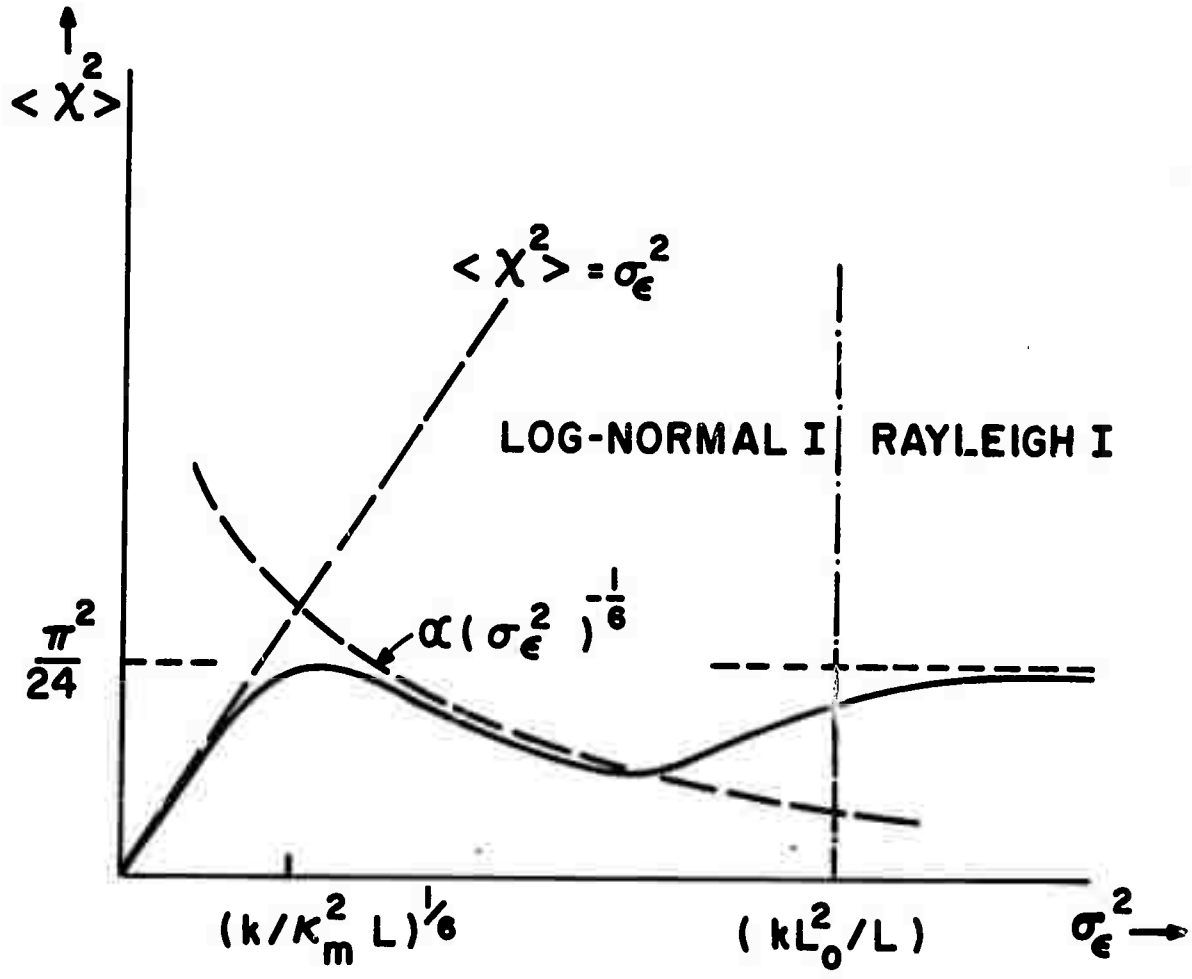

Figure 4. Log-amplitude variance $<\chi^2>$ vs $\sigma_\epsilon^2 \sim k^{7/6} L^{11/6} Cn^2$: A sample curve fitting the (dashed) asymptotes given by theory.

exaggeration [it may or may not occur, depending upon the magnitude of the coefficient of $(\sigma_\epsilon^2)^{-1/6}$]. The major weakness of the theory is its

inability to predict the coefficient of $(\sigma_\epsilon^2)^{-1/6}$ in $\langle \chi^2 \rangle$ in the saturation limit. The maximum of $\langle \chi^2 \rangle$ is therefore also not predictable in the present form of this work.

APPENDIX: SATURATION-REGIME LOG-AMPLITUDE VARIANCE

The result of section III for the saturation regime was,

$$< I^N > = I_o^N \exp[2N(N-1)< \delta\chi^2 >],$$

$$2<\delta\chi^2> = (k\epsilon/4\pi)^2 \int_o^L dz \int d^2K \Phi(K)\{1-\cos[K^2(L-z)/k]\} \qquad \text{(A1)}$$

$$x < \cos[\underset{\sim}{K}\cdot\Delta\underset{\sim}{\rho}(z)]> .$$

Here, it will be argued that $\Delta\underset{\sim}{\rho}(z)$ is the difference of two ray-coordinate realizations, and a first-order estimate of $< \delta\chi^2 >$ will be given. In order to determine the nature of $\Delta\underset{\sim}{\rho}(z)$ we will rederive (A1) in another fashion by regarding the equation for $\psi = \ln B$ obtained from the parabolic wave equation,

$$2ik\, \partial\psi/\partial z + \Delta_T\psi + k^2\delta\epsilon + (\underset{\sim}{\nabla}_T\psi)^2 = 0 . \qquad \text{(A2)}$$

The Rytov approximation (2) results when the last term of (A2) is dropped. We will follow a procedure analogous to that described in [4] to circumvent the difficulty of the last term. Let $\psi = \chi + i\varphi$. We obtain the ray equation $kd\underset{\sim}{\rho}(z)/dz = \underset{\sim}{\nabla}_T\psi$ from (4) by modifying the stationary-phase method to the more precise steepest-descent approximation [4]. Consider the transformation from the cartesian coordinate system (x,y,z) to the locally orthogonal curvilinear system $(\underset{\sim}{\rho}(s),s)$. It is easily seen that $\underset{\sim}{\nabla}_T\psi = 0$ in the new coordinate system; $\underset{\sim}{\nabla}_T\psi$ and $\Delta_T\psi$ are invariant with respect to the transformation and they may be expressed in any coordinate system. However $\partial\psi/\partial z$ is not invariant. Nevertheless, the curvilinear effects can be ignored in $\partial\psi/\partial z$ because the difference between $\partial\psi/\partial z$ and $\partial\psi/\partial s$ is $O(\kappa_m^{1/3} L C_n^2)$ as given by (11). Thus to good approximation

$$2ik\,\partial\psi/\partial s + \Delta_T\psi + k^2\delta\varepsilon = 0 \qquad \text{(A3)}$$

along rays determined by $k\,d\underset{\sim}{\rho}(z)/dz = \underset{\sim}{\nabla}_T\psi$ in terms of the original coordinate system. By utilizing $\delta\varepsilon(s) = \delta\varepsilon(\underset{\sim}{\rho}(z),z)$ and by replacing $dz \approx ds$ and $(L-s) \approx (L-z)$ we write the solution of (A3) as,

$$\psi = (ik/8\pi^2)\int_0^L dz \int d\underset{\sim}{\chi}(\underset{\sim}{K},z)\exp\{-i\underset{\sim}{K}\cdot[\underset{\sim}{\rho}(z)+(L-z)\underset{\sim}{K}/2k]\} \quad . \qquad \text{(A4)}$$

Eq. (A4) constitutes an important correction to (2), even in the limit $\rho \to 0$, because $\langle\psi\rangle \neq 0$. Tatarski, in a slightly different formulation [21] has computed $\langle\chi\rangle$ in the geometrical-optics regime where $\sin[K^2(L-z)/2k]$ may be replaced by $K^2(L-z)/2k$. It is this difference with (2) that yields the first equation in (A1), where $\langle\delta\chi^2\rangle$ represents the variance of $\chi = \mathrm{Re}\psi$. The derivation of (34) ensures the conservation law $\langle\chi\rangle + \langle\delta\chi^2\rangle = 0$ so that it suffices to compute one of these two quantities. If $\langle\delta\chi^2\rangle$ is formed from (A4) by subtracting $\langle\chi\rangle^2$ from $\langle\chi^2\rangle$, we obtain (A1) because the correlation between $d\underset{\sim}{\chi}(\underset{\sim}{K}_1,z_1)$ and $\underset{\sim}{\rho}(z_2)$ can be ignored (note that the multivariate Gaussian, or Markov, property holds for these quantities, e.g., as in paragraph 65 of [16]). The modified-Rytov approximation (21) follows by setting $\Delta\underset{\sim}{\rho}(z) = 0$.

The above procedure clearly is an improvement upon the customary Rytov approximation. However (A4) is valid beyond the region in which $\sigma_1^2 \ll 1$. It breaks down when σ_2^2, given by (29), approaches unity because the WKB expression for phase is significantly different from the straightened-ray expression. This can be seen from (A4) by ignoring the filter factor and repeating the estimate of (23a) with $\Delta QL/k$ replaced

by $\Delta\rho$ (with variance $\sim K_m^{1/3} L^3 C_n^2$). Thus, accepting the validity of (A4) for $\sigma_2^2 \ll 1$, we find (A1) from (A4) as described above. By comparing the result of this method to (33) we have been able to identify the hitherto unspecified $\underset{\sim}{\Delta\rho}(z)$ with the difference of two ray-coordinate realizations.

Now an estimate of $\langle \delta\chi^2 \rangle$ can be given. In (A1) we set $\langle \cos[\underset{\sim}{K}\cdot\underset{\sim}{\Delta\rho}(z)] \rangle = \exp[-K^2 \langle \Delta\rho^2(z) \rangle /4]$ by utilizing the Gaussian property of $\underset{\sim}{\Delta\rho}$. Furthermore, we insert $\epsilon^2\Phi(K) \approx 32\pi\gamma C_n^2 K^{-11/3}$ from (25) into (A1), transform variable K into $x = K^2(L-z)/k$, to obtain

$$\langle \delta\chi^2 \rangle = \gamma k^{7/6} C_n^2 \int_0^L dz z^{5/6} \int_0^\infty dx x^{-11/6} (1-\cos x) \exp[-xk \langle \Delta\rho^2(z) \rangle /4(L-z)] , \tag{A5}$$

where coefficient $\gamma \approx 0.033\pi^2$. The major problem is to compute $\langle \Delta\rho^2(z) \rangle$. The ray coordinates $\underset{\sim}{\rho}(z)$ converge to $\underset{\sim}{\rho}(L) = 0$ and diverge randomly as L-z grows. Considering the fact that the integrand of (A1) is negligible for $L-z \to 0$, we shall approximate $\langle \Delta\rho^2(z) \rangle \approx 4\langle \rho^2(z) \rangle$ as if both ray realizations are independent. This approximation should be better for large L, i.e. for large σ_1^2. We utilize the well-known geometrical-optics expression for $\langle \rho^2(z) \rangle$ given by Tatarski [21] when $\underset{\sim}{\rho}(L) = 0$ and ray derivative $\underset{\sim}{\rho}'(0) = 0$,

$$\langle \rho^2(z) \rangle = (4\gamma/3) C_n^2 K_m^{1/3} [(L-z)^3 + 3z(L-z)^2] \tag{A6}$$

to obtain,

$$\langle \delta\chi^2 \rangle = \gamma C_n^2 k^{7/6} L^{11/6} \int_0^1 dy y^{5/6} \int_0^\infty dx x^{-11/6} (1-\cos x) \exp[-x\sigma_1^2 f(y)]$$
$$f(y) \equiv (4\gamma/3)(1-y)(1+2y) , \tag{A7}$$

and $\sigma_1^2 = kL^2\kappa_m^{1/3}C_n^2$ in agreement with (29). It can be seen that $<\delta\chi^2>$ reduces to $\sigma_\epsilon^2 = 0.31k^{7/6}L^{11/6}C_n^2$ in the limit $\sigma_1^2 \to 0$. In order to obtain an expression for large σ_1^2, we return to (A1) and partially integrate {....} with respect to z. Upon utilizing the approximations incorporated into (A6) and (A7) we obtain

$$<\delta\chi^2> = \gamma C_n^2 k^{7/6} L^{11/6} \{ \int_0^\infty dx x^{-11/6}(1-x^{-1}\sin x)\exp(-\tfrac{4}{3}\gamma\sigma_1^2 x)$$

$$+ 8\gamma\sigma_1^2 \int_0^1 dy y(1-y) \int_0^\infty dx x^{-5/6}[1 - \frac{\sin(x(1-y))}{x(1-y)}]\exp[-x\sigma_1^2 f(y)]\} \qquad \text{(A8)}$$

For large σ_1^2, it is permissible to replace the filter factors in each term of (A8) by the x^2 term of their power-series expansion. It can be seen from the ensuing expression that the leading terms of (A8) for large σ_1^2 yield the dependence.

$$<\delta\chi^2> = \sigma_\epsilon^2 \cdot O(\sigma_1^2)^{-7/6}$$

which we have utilized in (34). The numerical coefficient can be computed from (A8), but it may only have an approximate meaning in view of the approximation $<\Delta\rho^2(z)> \approx 4<\rho^2(z)>$.

Note: A revised version of pp. 9-43 is currently being prepared for publication.

REFERENCES

[1] V. I. Tatarski, Sov. Phys.-JETP 29, 1133 (1969).

[2] D. A. de Wolf, J. Opt. Soc. Am. 58, 461 (1968).

[3] D. A. de Wolf, Radio Science 2, 1379 (1967); errata: 3, 308 (1968).

[4] D. A. de Wolf, J. Opt. Soc. 59, 1455 (1969).

[5] M. I. Sancer and A. D. Varvatsis, J. Opt. Soc. Am. 60, 654 (1970).

[6] W. P. Brown, Jr., J. Opt. Soc. Am. 61, 981 (1971).

[7] A. T. Young, J. Opt. Soc. Am. 60, 1495 (1970).

[8] J. F. Molyneux, J. Opt. Soc. Am. 61, 248 and 369 (1971).

[9] W. P. Brown, Jr., J. Opt. Soc. Am. 62, 45 (1972).

[10] K. Furutsu, J. Opt. Soc. Am. 62, 240 (1972).

[11] Y. N. Barabanenkov, Y. A. Kravtsov, S. M. Rytov, and V. I. Tatarski, Sov. Phys.-Uspekhi 13, 551 (1971).

[12] I. M. Dagesmanskaya and V. I. Shishov, Izv. Vysshikh Uchebn. Zavedenii-Radiofiz. 13, 16 (1970).

[13] K. S. Gochelashvily and V. I. Shishov, Optica Acta 18, 313 (1971), (a more recent communication has not appeared in print at the time of writing).

[14] G. Modesitt, J. Opt. Soc. Am. 61, 797 (1971).

[15] W. P. Brown, Jr., Coherent field in a random medium-effective refractive index, in Modern Optics, Ed. J. Fox, 717 (Polytechnic Press, Brooklyn, N. Y., 1967).

[16] V I. Tatarski, The Effects of the Turbulent Atmosphere on Wave Propagation, transl. for NOAA by Israel Program for Scientific Translations (Jerusalem 1971), available from U.S. Dept. of Commerce, NTIS, Springfield, Va. 22151.

[17] V. I. Klyatskin in a recent paper [Sov. Phys.-JETP 33, 703 (1971)] has come to the different conclusion that $\langle I^N \rangle \to N\langle I \rangle^N$ as $\sigma_\epsilon^2 \to \infty$, and that no probability distribution exists in this limit. This conclusion appears not valid for optical wave propagation in turbulent air for the following reasons: The limit $\sigma_\epsilon^2 \to \infty$ violates either the no-diffusion approximation $K_m^{1/3} L C_n^2 \ll 1$ implicit in the parabolic wave equation, or the smallness of the macroscale Fresnel number L/kL_o^2, or it corresponds to the trivial case $k \to \infty$. Klyatskin's treatment ignores the effect of macroscale L_o, hence it deals with an infinite-macroscale medium. In that case it is not surprising that the Rayleigh limit (see Section IV) is not found. For the then non-trivial case that k is finite Klyatskin's result can only hold for an infinite-macroscale medium in which $C_n^2 L$ is finite but $C_n^2 L^{7/6} \to \infty$; a clear impossibility because C_n^2 must be independent of L. If on the other hand, we allow $k \to \infty$, it is physically obvious that the free-space irradiance I_o must result.

[18] G. E. Mevers, M. P. Keister, Jr., and D. L. Fried, J. Opt. Soc. Am. 59, 491 (1969).

[19] R. H. Kleen and G. R. Ochs, J. Opt. Soc. Am. 60, 1695 (1970).

[20] M. E. Gracheva, Izv. Vysshikh Uchebn. Zavedenii-Radiofiz. 10, 775 (1967).

[21] V. I. Tatarski, Izv. Vysshikh Uchebn. Zavedenii-Radiofiz. 10, 48 (1967).